Quantum Tomography in Neutral Meson and Antimeson Systems

Kun Cheng,[1,*] Tao Han,[1,†] Matthew Low,[1,‡] and Tong Arthur Wu[1,§]

[1] *PITT PACC, Department of Physics and Astronomy, University of Pittsburgh, 3941 O'Hara St., Pittsburgh, PA 15260, USA*

(Dated: July 11, 2025)

The flavor space of particles produced in collider environments contains informative quantum correlations. We present a systematic approach for constructing the complete flavor density matrix for a meson and antimeson system ($M\bar{M}$) in the Bloch vector space at a given time t, which can be at or after production. We point out that the B_s^0 and K^0 systems are superior to the B_d^0 and D^0 systems for quantum tomography because of their flavor oscillation and decay properties. Performing quantum tomography for the $M\bar{M}$ system can facilitate the study of production mechanisms, decoherence phenomena, quantum information variables, and potential new sources of CP violation.

Introduction

Ever since the original quantum mechanical formulation of $K^0\bar{K}^0$ mixing [1], systems of a neutral meson M and its antimeson $\bar{M}$ ($M\bar{M}$) have demonstrated many aspects of fundamental physics, such as the superposition of quantum states and the uncertainty principle. These systems also probe physics at an energy scale much above the neutral meson masses through quantum loop effects. They have provided us with enriched laboratories that advance our understanding of quark masses, their flavor mixing, CP violation, as well as constraining new physics beyond the Standard Model (SM) [2].

Due to the mixing between a meson and an antimeson, a meson state may be intrinsically treated as a qubit in flavor space. Pairs of oscillating mesons correspond to two-qubit systems that have been studied for various different mesons [3–17]. Attempts to observe entanglement and Bell nonlocality have been made, including in the $K^0\bar{K}^0$ system from resonant ϕ decay [3–5], and in the $B_d^0\bar{B}_d^0$ system from the decay of the $\Upsilon(4S)$ particle [6, 7]. In these cases, the initial state has the definitive quantum numbers $J^{PC} = 1^{--}$, which means that the flavor state of the meson pair is a maximally entangled state as dictated by symmetry. The existing results, however, focus mostly on comparing quantum and classical predictions and have limited use for quantum information.

In this work, we show how to reconstruct the most general two-particle flavor quantum state at an arbitrary time after production. We focus on the semi-leptonic decay channels in both the $B_s^0\bar{B}_s^0$ and $K^0\bar{K}^0$ systems, using the total semi-leptonic decay rate and the flavor asymmetry to form a complementary set of measurements of the flavor state. Based on the intrinsic properties of flavor oscillations and decays, we identify the optimal systems as B_s^0 and K^0 for quantum tomography. Using the observables we derive, we show that it is possible to fully measure the quantum properties of the flavor state of the meson pair, thus enabling quantum-state tomography systematically in flavor space for the first time. This work is largely orthogonal and complementary to the recent work on spin quantum tomography [18–21].

When a heavy quark pair originates from open flavor production at colliders, via the strong or electromagnetic interactions, the corresponding heavy hadrons are initially in flavor eigenstates. In general, however, the flavor correlation of the pair of hadronic states cannot be determined from first principles because of the non-perturbative hadronization process. Developing an approach for quantum tomography in this system may therefore provide an opportunity to study the underlying hadronization mechanisms [22].

The demonstration of flavor quantum tomography not only makes all quantum information measurements, such as concurrence, quantum discord, and quantum entropies available in the flavor sector, but also provides a crucial reference for theoretical predictions of the flavor state production from non-perturbative processes, as well as potential observations of new sources of CP violation.

Flavor Quantum States and Time-Evolution

When a meson is neutral under gauge symmetries, the meson state $|M\rangle$ mixes with the antimeson state $|\bar{M}\rangle$. Examples of neutral mesons M include B_d^0, B_s^0, D_d^0, D_s^0, and K^0. In the flavor space spanned by $|M\rangle$ and $|\bar{M}\rangle$, a single meson can be analyzed as a two-level quantum system [1], known as a qubit, and described with a density matrix $\rho_{_M}$. This matrix can be parameterized as

$$\rho_{_M} = \frac{\mathbb{1}_2 + b_i\sigma_i}{2}, \tag{1}$$

where $\mathbb{1}_2$ is the two-dimensional identity matrix and σ_i ($i = x, y, z$) are the Pauli matrices, with repeated indices summed over. The real vector b_i, known as the Bloch vector, specifies a quantum state in the Bloch vector space [23, 24].

With a common mass m and a common decay width Γ for the meson and antimeson, the non-Hermitian effective Hamiltonian is

$$\mathcal{H} = \mathbf{M} - i\mathbf{\Gamma}/2 = \begin{pmatrix} m - i\frac{\Gamma}{2} & H_{12} \\ H_{21} & m - i\frac{\Gamma}{2} \end{pmatrix}, \tag{2}$$

* kun.cheng@pitt.edu
† than@pitt.edu
‡ mal431@pitt.edu
§ tow39@pitt.edu

where H_{12} and H_{21} are complex parameters that characterize meson-antimeson mixing. Diagonalizing Eq. (2) yields the mass eigenstates $|M_1\rangle$ and $|M_2\rangle$, along with their masses and decay widths:

$$|M_1\rangle = p|M\rangle + q\left|\bar{M}\right\rangle, \qquad \text{with } (m_1,\, \Gamma_1), \tag{3}$$
$$|M_2\rangle = p|M\rangle - q\left|\bar{M}\right\rangle, \qquad \text{with } (m_2,\, \Gamma_2), \tag{4}$$

where $|q|^2 + |p|^2 = 1$ and $p/q = \sqrt{H_{12}/H_{21}}$. In the absence of CP violation $p = q = 1/\sqrt{2}$. We adopt the convention $\mathrm{CP}|M\rangle = \left|\bar{M}\right\rangle$, implying that $|M_1\rangle$ is a CP-even eigenstate and $|M_2\rangle$ is CP-odd. In the Bloch vector space, the flavor eigenstates $|M\rangle$ and $\left|\bar{M}\right\rangle$ are described by $\vec{b} = (0,0,\pm 1)$ while the mass eigenstates $|M_1\rangle$ and $|M_2\rangle$ are described by $\vec{b} = (\pm 1,0,0)$.

Since the meson or antimeson can decay, as evidenced by their non-zero widths, this is an open quantum system that can be effectively described by non-unitary time evolution $U(t)$ [9, 25–27],

$$U(t) = \begin{pmatrix} \frac{1}{2}(e^{-\Gamma_1 t/2 - im_1 t} + e^{-\Gamma_2 t/2 - im_2 t}) & \frac{q}{2p}(e^{-\Gamma_1 t/2 - im_1 t} - e^{-\Gamma_2 t/2 - im_2 t}) \\ \frac{p}{2q}(e^{-\Gamma_1 t/2 - im_1 t} - e^{-\Gamma_2 t/2 - im_2 t}) & \frac{1}{2}(e^{-\Gamma_1 t/2 - im_1 t} + e^{-\Gamma_2 t/2 - im_2 t}) \end{pmatrix}. \tag{5}$$

where $U(t)$ is expressed in the flavor basis. The fraction of remaining mesons at time t is

$$\frac{N(t)}{N_0} = \mathrm{tr}\big(U(t)\rho_{_M}U(t)^\dagger\big), \tag{6}$$

where N_0 is the number of mesons at $t = 0$ and $N(t)$ is the number of mesons left at time t. The explicit form of $N(t)$ is given in Appendix A. For the rest of this work, we take $t = 0$ as the time of production, though one can choose any starting point as $t = 0$.

The time evolution of the quantum density matrix, in the Schrödinger picture, is

$$\rho_{_M}(t) = \frac{U(t)\rho_{_M}U(t)^\dagger}{\mathrm{tr}\big(U(t)\rho_{_M}U(t)^\dagger\big)}. \tag{7}$$

The normalization of $\rho_{_M}(t)$ leads to unitary evolution.

The Oscillation and Decay of Bloch Vectors

It is intuitive to analyze the state evolution in the Bloch vector space [23, 24], because different components of the quantum density matrix $\rho_{_M}$ are probed by the various decays of the neutral meson, as we formulate explicitly below. The time evolution of the Bloch vector is [26, 28, 29]

$$\frac{d}{dt}\vec{b}(t) = -2\vec{E}\times\vec{b}(t) + \vec{\Gamma} - [\vec{\Gamma}\cdot\vec{b}(t)]\,\vec{b}(t), \tag{8}$$

where the vectors $\vec{E}$ and $\vec{\Gamma}$ are defined from the decompositions of the Hermitian matrices $\mathbf{M}$ and $\mathbf{\Gamma}$ in Eq. (2) as

$$\mathbf{M} = E_0\mathbb{1}_2 + \vec{E}\cdot\vec{\sigma}, \qquad \mathbf{\Gamma} = \Gamma_0\mathbb{1}_2 + \vec{\Gamma}\cdot\vec{\sigma}. \tag{9}$$

In this paper, we work in the CP-conserving limit with

$$H_{21} = H_{12} = \frac{\Delta m}{2} + i\frac{\Delta\Gamma}{4}, \tag{10}$$

where $\Delta m \equiv m_2 - m_1$ and $\Delta\Gamma = \Gamma_1 - \Gamma_2$. Therefore, both vectors $\vec{E} = (\Delta m/2,0,0)$ and $\vec{\Gamma} = (-\Delta\Gamma/2,0,0)$ point along the $\vec{x}$ direction.

Collapse to Flavor Eigenstates – Consider a multi-particle final state $|f\rangle$ with $\mathrm{CP}|f\rangle = \left|\bar{f}\right\rangle$ and $|f\rangle \neq \left|\bar{f}\right\rangle$. In the CP-conserving limit, the meson M only decays to f while the antimeson $\bar{M}$ only decays to $\bar{f}$. The semi-leptonic decays of neutral mesons are examples of such decays. The observation of such decays identifies the flavor of the neutral meson as $|M\rangle$ or $\left|\bar{M}\right\rangle$. The probabilities of collapsing the meson state to flavor eigenstates are

$$\langle M|\,\rho_{_M}(t)\,|M\rangle = \frac{1+b_z(t)}{2}, \quad \left\langle\bar{M}\right|\rho_{_M}(t)\left|\bar{M}\right\rangle = \frac{1-b_z(t)}{2}.$$

Let $N_{f/\bar{f}}(t)$ be the number of $f/\bar{f}$ final states produced in decays from $t = 0$ until time t. The rate of change is

$$\frac{d}{dt}N_{f/\bar{f}}(t) = N(t)\frac{1\pm b_z(t)}{2}\Gamma_{M\to f}, \tag{11}$$

where $\Gamma_{M\to f}$ is the partial width of M decaying to f and $\Gamma_{M\to f} = \Gamma_{\bar{M}\to\bar{f}}$.

In practice, we propose to measure the decay asymmetry $N_f(t) - N_{\bar{f}}(t)$, which directly corresponds to the expectation value of σ_z with $\mathrm{Tr}\big(\sigma_z\cdot\rho_{_M}(t)\big) = b_z(t)$,

$$\begin{aligned}\frac{d(N_f(t) - N_{\bar{f}}(t))}{dt} &= N(t)b_z(t)\Gamma_{M\to f}, \\ &= N_0\,e^{-\Gamma t}(b_z\mathrm{c}_t - b_y\mathrm{s}_t)\Gamma_{M\to f}.\end{aligned} \tag{12}$$

where $\mathrm{c}_t = \cos(\Delta m t)$, $\mathrm{s}_t = \sin(\Delta m t)$, and $b_i = b_i(0)$ are the components of the Bloch vector at $t = 0$. The decay asymmetry probes both b_y and b_z as they evolve into each other according to Eq. (8), which describes precession around the x direction in the limit of $\Delta m \gg \Gamma$. Therefore, when decays occur at different times, this allows us to measure different directions in the $y-z$ plane of the Bloch vector space.

In the Heisenberg picture, the Bloch vector $\vec{b}(0)$ does not rotate. Instead, the asymmetry operator σ_z oscillates with σ_y. Measuring decays at different times probes the operator at different times and maps out the y and z components of the Bloch vector at $t = 0$.

Collapse to CP eigenstates – The neutral mesons can also decay to CP eigenstates with $|f_{\eta_{CP}}\rangle = \mathrm{CP}\,|f_{\eta_{CP}}\rangle = \eta_{CP}\,|f_{\eta_{CP}}\rangle$, where $\eta_{CP} = \pm 1$ is the CP eigenvalue of the final state $|f_{\eta_{CP}}\rangle$. The decays of $B_s^0 \to J/\psi\eta$ and $K^0 \to \pi^+\pi^-$ are such examples. Instead of collapsing the meson state to $|M\rangle$ or $|\bar{M}\rangle$, the decay to $|f_{\eta_{CP}}\rangle$ collapses the meson state to the CP eigenstates (or mass eigenstates) $|M_1\rangle$ or $|M_2\rangle$, whose Bloch vectors are along the x direction.[1] Such decays allow the reconstruction of b_x.

Due to the uneven decay rates of the CP-odd and CP-even states, there is no simple asymmetric observable directly corresponding to $\langle\sigma_x\rangle$ as in Eq. (12). However, the decay can still be viewed as a projection to $|M_1\rangle$ and $|M_2\rangle$ with[2]

$$\langle M_1|\,\rho_{_M}(t)\,|M_1\rangle = \frac{1+b_x(t)}{2},\ \langle M_2|\,\rho_{_M}(t)\,|M_2\rangle = \frac{1-b_x(t)}{2},$$

and one can reconstruct b_x from such decay. The decay rate to f_+ of a meson at time t is

$$\Gamma_{M(t)\to f_+} = \frac{1+b_x(t)}{2}\Gamma_{M_1\to f_+} = (1+b_x(t))\Gamma_{M\to f_+},$$

where $\Gamma_{M\to f_+} = \frac{1}{2}\Gamma_{M_1\to f_+}$ is because $|M\rangle = (|M_1\rangle + |M_2\rangle)/\sqrt{2}$ and only $|M_1\rangle$ decays to f_+. Therefore, the x component of the Bloch vector can be reconstructed from the decay to CP eigenstates. Furthermore, the decay to CP eigenstates results in a decay width difference $\Delta\Gamma = \Gamma_1 - \Gamma_2$ and lifetime difference, leading to the b_x dependence in the decay rate to the total flavor eigenstates, both f and $\bar{f}$, as a function of time

$$\begin{aligned}\frac{d(N_f(t)+N_{\bar{f}}(t))}{dt} &= N(t)\Gamma_{M\to f}\\ &= N_0\, e^{-\Gamma t}(\mathrm{ch}_t - b_x \mathrm{sh}_t)\Gamma_{M\to f},\end{aligned} \quad (13)$$

where $\mathrm{ch}_t = \cosh(\Delta\Gamma t/2)$ and $\mathrm{sh}_t = \sinh(\Delta\Gamma t/2)$. Thus, one can fully reconstruct $b_{x,y,z}$ by only measuring the $M \to f/\bar{f}$ decay channels and comparing these observables with Eqs. (12) and (13).

To summarize, the components of the Bloch vector in the $y-z$ plane are probed by the flavor asymmetry $N_f - N_{\bar{f}}$ via oscillations in Eq. (12), and the Bloch vector in the x direction is measured from $N_f + N_{\bar{f}}$ via total decay rates in Eq. (13). By fitting the distributions of $N_f \pm N_{\bar{f}}$ with respect to decay time, the complete flavor density matrix for a single meson is reconstructed.

Generalization to Meson Pairs – The quantum state of a two-meson system, with the two subsystems denoted as $\mathcal{A}$ and $\mathcal{B}$, respectively, can be expressed by the density matrix

$$\rho_{_{MM}} = \frac{\mathbb{1}_4 + b_i^{\mathcal{A}}\sigma_i\otimes\mathbb{1}_2 + b_i^{\mathcal{B}}\mathbb{1}_2\otimes\sigma_i + C_{ij}\sigma_i\otimes\sigma_j}{4}, \quad (14)$$

where $b_i^{\mathcal{A}}$ and $b_i^{\mathcal{B}}$ describe the flavor state of mesons $\mathcal{A}$ and $\mathcal{B}$, respectively, and C_{ij} is the flavor correlation matrix between the two mesons. Repeated indices are summed over. Collectively, these are also called the Fano coefficients [30].

Similarly to the single meson case, for a meson pair as a two-qubit system, their Bloch vectors $b_i^{\mathcal{A}}$ and $b_i^{\mathcal{B}}$ and their correlation matrix C_{ij} are obtained by measuring the flavor asymmetry and the total decay rate to a flavor eigenstate, for each meson. This leads us to define the following four observables

$$N_{\mathrm{tot}} = N_{ff} + N_{\bar{f}f} + N_{f\bar{f}} + N_{\bar{f}\bar{f}}, \quad (15)$$

$$A_{ff} = N_{ff} - N_{\bar{f}f} - N_{f\bar{f}} + N_{\bar{f}\bar{f}}, \quad (16)$$

$$A_f^{\mathcal{A}} = N_{ff} - N_{\bar{f}f} + N_{f\bar{f}} - N_{\bar{f}\bar{f}}, \quad (17)$$

$$A_f^{\mathcal{B}} = N_{ff} + N_{\bar{f}f} - N_{f\bar{f}} - N_{\bar{f}\bar{f}}, \quad (18)$$

where $N_{f_1 f_2}$ is the number of events in which meson $\mathcal{A}$ decays to f_1 and meson $\mathcal{B}$ decays to f_2. All quantities above depend on the times t_1 and t_2.

N_{tot} is the total number of events from semi-leptonic decays, A_{ff} is the asymmetry between like and unlike decays, and $A_f^{\mathcal{A}/\mathcal{B}}$ is the decay flavor asymmetry of one meson under the condition that the other meson also decays to a flavor eigenstate. The distributions of the four observables have the following dependence on the flavor density matrix of the meson pair (see Appendix B for details),

[1] When CP is not conserved the eigenstates of CP and of mass no longer coincide.

[2] Here we assumed $\langle M|f_+\rangle = \langle\bar{M}|f_+\rangle$ for illustration while our result Eq. (13) does not rely on this.

$$\frac{\mathrm{d}^2 N_{\rm tot}}{\mathrm{d}t_1 \mathrm{d}t_2} = N_0 \Gamma^2_{B_0\to f}\, e^{-\Gamma(t_1+t_2)} \big(\mathrm{ch}_{t_1}\mathrm{ch}_{t_2} - \mathrm{ch}_{t_1}\mathrm{sh}_{t_2} b_x^{\mathcal{A}} - \mathrm{sh}_{t_1}\mathrm{ch}_{t_2} b_x^{\mathcal{B}} + C_{xx}\mathrm{sh}_{t_1}\mathrm{sh}_{t_2}\big) + \mathcal{O}(\epsilon) \tag{19}$$

$$\frac{\mathrm{d}^2 A_{ff}}{\mathrm{d}t_1 \mathrm{d}t_2} = N_0 \Gamma^2_{B_0\to f}\, e^{-\Gamma(t_1+t_2)} \big(\mathrm{s}_{t_1}\mathrm{s}_{t_2} C_{yy} - \mathrm{c}_{t_1}\mathrm{s}_{t_2} C_{zy} - \mathrm{s}_{t_1}\mathrm{c}_{t_2} C_{yz} + \mathrm{c}_{t_1}\mathrm{c}_{t_2} C_{zz}\big) + \mathcal{O}(\epsilon) \tag{20}$$

$$\frac{\mathrm{d}^2 A_f^{\mathcal{A}}}{\mathrm{d}t_1 \mathrm{d}t_2} = N_0 \Gamma^2_{B_0\to f}\, e^{-\Gamma(t_1+t_2)} \big(\mathrm{ch}_{t_2}(\mathrm{c}_{t_1} b_z^{\mathcal{A}} - \mathrm{s}_{t_1} b_y^{\mathcal{A}}) - \mathrm{sh}_{t_2}(\mathrm{c}_{t_1} C_{zx} - \mathrm{s}_{t_1} C_{yx})\big) + \mathcal{O}(\epsilon) \tag{21}$$

$$\frac{\mathrm{d}^2 A_f^{\mathcal{B}}}{\mathrm{d}t_1 \mathrm{d}t_2} = N_0 \Gamma^2_{B_0\to f}\, e^{-\Gamma(t_1+t_2)} \big(\mathrm{ch}_{t_1}(\mathrm{c}_{t_2} b_z^{\mathcal{B}} - \mathrm{s}_{t_2} b_y^{\mathcal{B}}) - \mathrm{sh}_{t_1}(\mathrm{c}_{t_2} C_{xz} - \mathrm{s}_{t_2} C_{xy})\big) + \mathcal{O}(\epsilon) \tag{22}$$

where N_0 is the total number of $M\bar{M}$ events, t_1 and t_2 are the decay times of the first and second meson, and only the semi-leptonic decay channel is considered. Here, ϵ is the CP violation parameter in the $M\bar{M}$ mixing defined by $p/q = (1+\epsilon)/(1-\epsilon)$. For B_s^0, $\epsilon \sim \mathcal{O}(10^{-5})$, and for K^0, $\epsilon \sim \mathcal{O}(10^{-3})$. This justifies our analysis as a good approximation by ignoring the CP-violation effects. Another source of CP violation, the difference between the decay amplitudes of M and $\bar{M}$ when decaying to CP eigenstates [31, 32], is irrelevant to the four observables above. By measuring the four distributions, we reconstruct all the Fano coefficients $\vec{b}^{\mathcal{A}}$, $\vec{b}^{\mathcal{B}}$, and C_{ij}. Deviations from the predictions made by the density matrix parametrization may indicate the presence of decoherence phenomena [4, 5, 27].

Simulations and Experimental Feasibility

From an observational perspective, a $M\bar{M}$ system needs to have a sizable value of $\Delta m/\Gamma$ and $\Delta\Gamma/\Gamma$, ideally of order unity or larger. This corresponds to rapid oscillations and an appropriate decay lifetime difference.

As shown in Table III, B_s^0 system is such a system with $(\Delta m/\Gamma,\ \Delta\Gamma/\Gamma)_{B_s^0} = (27,\ 0.14)$. The B_d^0 system, with $(\Delta m/\Gamma,\ \Delta\Gamma/\Gamma)_{B_d^0} = (0.77,\ 0.004)$, does have a suitable oscillation time, but the decay lifetime difference is too small to be appreciable. Therefore, in this system, the $(2\times 2)_{yz}$ subset of the correlation matrix can be measured which is sufficient to measure the Bell nonlocality [6, 7], but full tomography cannot be performed because the small lifetime difference does not allow a usable measurement of b_x. The D^0 system has small values of both $\Delta m/\Gamma$ and $\Delta\Gamma/\Gamma$ which makes quantum tomography much more challenging. For the K^0 system both quantities are sizable, $(\Delta m/\Gamma,\ \Delta\Gamma/\Gamma)_{K^0} = (0.95,\ 1.99)$. We therefore adopt the B_s^0 and K^0 systems to quantitatively demonstrate the procedure of quantum tomography.

We choose two examples of density matrices for concreteness. The first is $\rho_{\rm Bell}$, parametrized as

$$b_i^{\mathcal{A}} = b_i^{\mathcal{B}} = 0 \quad \text{and} \quad C_{ij} = -\delta_{ij}, \tag{23}$$

which corresponds to the CP-odd flavor state $(|M\bar{M}\rangle - |\bar{M}M\rangle)/\sqrt{2}$. The second is the Werner state ρ_κ [33] given by

$$\rho_\kappa = (1-\kappa)\rho_{\rm Bell} + \kappa\frac{\mathbb{1}_4}{4}, \tag{24}$$

where $\mathbb{1}_4/4$ is a maximally mixed state and we use $\kappa = 0.2$.

The samples are distributed in the two-dimensional space (t_1, t_2) where t_1 and t_2 are the decay times of the first and second mesons, respectively. For each of the two states $\rho_{\rm Bell}$ and ρ_κ, we consider the binned distribution of $N_{\rm tot}$ from 10^7 semi-leptonically-decaying events. From this we extract N_0, $b_x^{\mathcal{A}}$, $b_x^{\mathcal{B}}$, and C_{xx} with Eq. (19). The extracted value of N_0 is then used when fitting to A_{ff}, $A_f^{\mathcal{A}}$ and $A_f^{\mathcal{B}}$, in Eqs. (20)−(22), to measure the coefficients $b_i^{\mathcal{A}}$, $b_i^{\mathcal{B}}$, and C_{ij}. The central value and statistical uncertainty of fitted results are estimated from the mean and the standard deviation of 40 pseudo-experiments.

The B_s^0 meson pair events are generated with $0 < t_1, t_2 < 3.5$ ps, within the first 10 periods of oscillation and about twice the mean lifetime. The oscillatory time evolution versus t_1 is shown in Fig. 1(a), integrated over a range of t_2 for the $\rho_{\rm Bell}$ initial state. We adopt a similar bin width as Ref. [34] with each period divided into 6 bins, leading to 60×60 bins in the $t_1 - t_2$ plane. We find that the density matrix can be effectively reconstructed in our formalism, as shown in Table I. The measurement precision of the C_{xx} entry of the flavor correlation matrix is much lower than the other coefficients, because the B_s^0 mesons have relatively small $\Delta\Gamma/\Gamma$ and the sensitivity of C_{xx} is suppressed by two factors of $\sinh(\Delta\Gamma t/2)$.

The analysis for K^0 meson pairs is similar. We generate events with $0 < t_1, t_2 < 0.59$ ns, within the first half-period of the damped oscillation and 6.7 times the lifetime of K_S, as shown in Fig. 1(b). We divide the half-period into 20 bins, similar to Ref. [35], which yields a total 20×20 bins. Although K^0 and $\bar{K}^0$ cannot completely evolve into each other before the quick K_S decay, the oscillation of about a quarter-period is still sufficient to construct b_y and b_z. With nearly maximal $\Delta\Gamma/\Gamma$, the sensitivity of C_{xx} coefficient is not suppressed in the K^0 system and can be reconstructed equally well as the other coefficients. Collecting events with decays extending to several times the K_S lifetime is enough to perform quantum tomography, although studying the K_L events at

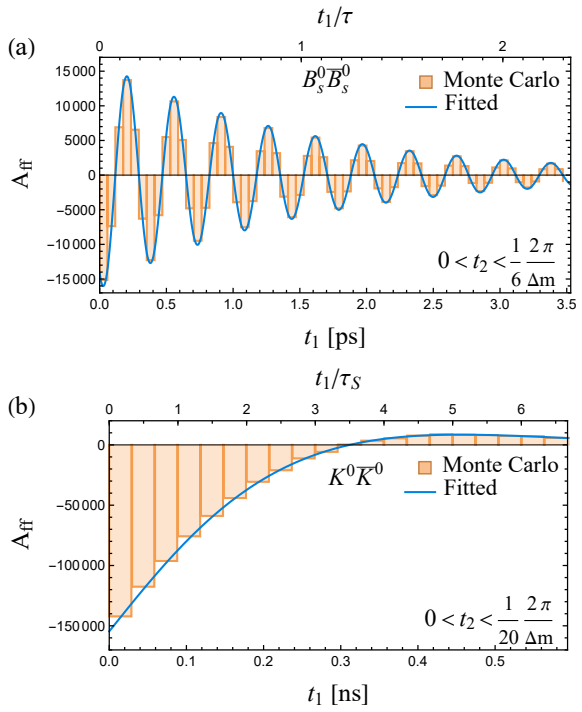

FIG. 1. Monte Carlo and fitted distribution of $A_{ff}(t_1,t_2)$ for $B_s^0\bar{B}_s^0$ and $K^0\bar{K}^0$, in the direction of t_1 with t_2 interval specified in the figure. The labels of the upper axes are the time in units of the decay lifetime of B_s^0 and K_S^0.

	$B_s^0\bar{B}_s^0$ fitted $\rho_{\rm Bell}$ (ρ_κ)	$K^0\bar{K}^0$ fitted $\rho_{\rm Bell}$ (ρ_κ)	Obs.
$b_x^{\mathcal{A}}$	0±0.020 (0±0.017)	0±0.0015 (0±0.0018)	$N_{\rm tot}$
$b_x^{\mathcal{B}}$	0±0.019 (0±0.016)	0±0.0017 (0±0.0018)	
$b_y^{\mathcal{A}}$	0±0.0009 (0±0.0010)	0±0.0019 (0±0.0021)	$A_f^{\mathcal{A}}$
$b_z^{\mathcal{A}}$	0±0.0010 (0±0.0009)	0±0.0014 (0±0.0016)	
$b_y^{\mathcal{B}}$	0±0.0010 (0±0.0008)	0±0.0020 (0±0.0023)	$A_f^{\mathcal{B}}$
$b_z^{\mathcal{B}}$	0±0.0009 (0±0.0008)	0±0.0015 (0±0.0016)	
C_{xx}	−1±0.36 (−0.8±0.29)	−1±0.0031 (−0.8±0.0032)	$N_{\rm tot}$
C_{yx}	0±0.016 (0±0.018)	0±0.0023 (0±0.0026)	$A_f^{\mathcal{A}}$
C_{zx}	0±0.018 (0±0.017)	0±0.0017 (0±0.0019)	
C_{xy}	0±0.017 (0±0.015)	0±0.0025 (0±0.0029)	$A_f^{\mathcal{B}}$
C_{xz}	0±0.016 (0±0.016)	0±0.0018 (0±0.0020)	
C_{yy}	−1±0.0011 (−0.8±0.0010)	−1±0.0027 (−0.8±0.0023)	A_{ff}
C_{yz}	0±0.0007 (0±0.0008)	0±0.0022 (0±0.0020)	
C_{zy}	0±0.0008 (0±0.0008)	0±0.0021 (0±0.0017)	
C_{zz}	−1±0.0011 (−0.8±0.0009)	−1±0.0010 (−0.8±0.0011)	

TABLE I. The central values and statistical uncertainties of the Fano coefficients in the $B_s^0\bar{B}_s^0$ system and in the $K^0\bar{K}^0$ system, using the initial states $\rho_{\rm Bell}$ and ρ_κ with $\kappa = 0.2$. Each system uses 10^7 events and 40 pseudo-experiments. The statistical uncertainties scale as $1/\sqrt{N}$.

later times is also fruitful in exploring quantum phenomena [4, 5].

Results are shown in Table I with 10^7 events. In practice, approximately 7×10^6 $B_s^0\bar{B}_s^0$ pairs have been produced at Belle [36, 37], and around 3×10^8 are expected to be produced at Belle II [38], mostly in pure Bell states from the decay of the $\Upsilon(5S)$.

At LHCb, a pair of B_s^0 mesons can be produced from the hadronization of $b\bar{b}$, which has a cross section of $\sigma(b\bar{b}X) = 0.56$ mb [39], and a fraction of around 1.4% [40] goes to a pair of B_s^0 mesons. With the Run 2 luminosity of 5.7 fb^{-1}, there are 8×10^{10} $B_s^0\bar{B}_s^0$'s produced. The fraction of both B_s^0's decaying semi-leptonically is $\mathrm{Br}(B_s^0\to\ell^+\nu_\ell X^-)^2 = 3.7\%$, which potentially yields as many events as our sample simulation. The reconstruction of a pair of b-hadrons has been discussed in Ref. [41], and we expect a similar efficiency. Due to the complicated nature of production and hadronization in hadronic collisions, it is unclear to what extent a B^0 meson pair would be flavor-entangled, which will be an interesting subject to explore theoretically and experimentally.

K^0 is typically pair produced from ϕ meson decay. Around 8×10^9 $K^0\bar{K}^0$ pairs have been produced at KLOE and KLOE-2 [42], and a fraction of 1.1% decays in $0 < t < \pi/\Delta m$, among which a fraction of $\mathrm{BR}(K_S^0\to\pi^\pm\ell^\mp\nu_\ell)\mathrm{BR}(K_L^0\to\pi^\pm\ell^\mp\nu_\ell) = 8\times10^{-4}$ decays to leptons on both side.

Applications to Quantum Information

Having performed quantum tomography for the $M\bar{M}$ system, we are in a position to study any quantum information observable of the system. We list the definitions of some example quantities in Appendix C.

Concurrence is a measure of the entanglement of a system which measures how much the two subsystems are not separable [43]. The Bell variable is a normalized measurement of Bell inequality where a positive value signifies that a local hidden variable model cannot imitate this result [44]. Quantum discord is a weaker correlation than entanglement [45, 46]. A non-zero value of discord indicates that the system is not invariant under measurements, which is one of the prime features of quantum systems. A positive value of steerability indicates that the system cannot be described by a local hidden state model. Conditional entropy quantifies the number of bits needed for subsystem $\mathcal{A}$ to reconstruct subsystem $\mathcal{B}$. Classically, this is restricted to non-negative values, but quantum mechanically negative values are possible [47]. The second stabilizer Rényi entropy (SSRE) is a measure of the magic of a quantum system which quantifies the computation advantage this system would have over a classical computer [48].

These quantities are listed in Table II for ρ_κ with $\kappa = 0.2$. All quantities can be measured to a high precision. For quantities that require the full density matrix for their calculation, their precision is limited by the

largest uncertainty in Table I. Some quantities, however, only require a subset of the Fano coefficients, like Bell nonlocality, in which case it can often be measured to higher precision.

	$B_s^0\bar{B}_s^0$	$K^0\bar{K}^0$
Concurrence	0.69 ± 0.14	0.702 ± 0.0024
Bell Variable	0.1854 ± 0.0014	0.188 ± 0.003
Quantum Discord	0.58 ± 0.10	0.617 ± 0.0023
Steerability Variable	0.48 ± 0.07	0.4822 ± 0.0015
Conditional Entropy	-0.15 ± 0.29	-0.157 ± 0.005
SSRE	0.38 ± 0.15	0.388 ± 0.003

TABLE II. Reconstructed quantum information quantities for ρ_κ with $\kappa = 0.2$.

Conclusion and Outlook

The flavor space of particles produced in collider environments provides quantum information as rich as that of the spin space. Expressing the flavor density matrix for a neutral meson M by the Pauli matrices in the Bloch vector space, we constructed the flavor correlation matrices for the $M\bar{M}$ system at a given time t. The crucial observations are that different components in flavor space are related to different physical observables. Defining the flavor eigenstates along the z-direction, the y and z components are measured from the oscillation of the flavor asymmetry, with a sensitivity related to the mass difference Δm. The x components are measured from the time dependence of the total semi-leptonic decay rate, with a sensitivity related to the decay lifetime difference $\Delta\Gamma$.

Our analysis provides a systematic way to construct the complete flavor density matrix for a $M\bar{M}$ system, and study its production mechanisms, decoherence phenomena, and quantum properties. From the observational point of view, meson systems with suitable $\Delta m/\Gamma$ and $\Delta\Gamma/\Gamma$ are required. We observed that the B_s^0 and K_S^0 systems are superior to the B_d^0 and D^0 systems due to their favorable oscillation and decay properties. Through numerical simulations, we demonstrated that the full density matrices can be precisely reconstructed, as shown in Fig. 1 and Table I. Through the procedure of quantum tomography, one can construct any quantum information variable, such as concurrence, quantum discord, steerability, and magic, as shown in Table II.

A few final remarks are in order. First, as pointed out in Refs. [49–51], testing the nonlocality with the meson pair as an open system is not in a rigorous EPR sense. Instead, the goal of this work is to reconstruct the complete flavor density matrix of the meson pairs at a given time t at or after they are produced, and study their quantum information. Second, although the overall effects are rather small, the CP-violating interactions in the mixing would change the precession feature in the state evolution, and therefore introduce additional modulation in the observables. The flavor asymmetry observables would involve all of the 3×3 elements of the flavor correlation matrix instead of only the y and z components. Precision tomography could thus be sensitive to new CP violating sources. Thirdly, for meson pairs from quark hadronization, there is no first-principles calculation of the flavor state. Our formalism assumes the most general $M\bar{M}$ quantum state to begin with as in Eq. (14). This provides a new avenue to explore hadronization mechanisms in terms of quantum correlations, both theoretically and experimentally.

Overall, we demonstrated that performing quantum tomography for the $M\bar{M}$ system can facilitate the study of production mechanisms, decoherence phenomena, quantum information variables, and potential new sources of CP violation.

ACKNOWLEDGMENTS

We thank Alex Lenz, Zoltan Ligeti and Fabio Maltoni for discussions. This work was supported in part by the U.S. Department of Energy under grant No. DE-SC0007914 and in part by the Pitt PACC. ML is also supported by the National Science Foundation under grant No. PHY-2112829.

Appendix A: The Time Evolution of Single Meson

Consider the density matrix $\rho_{_M}$ for a single meson at time $t = 0$. The time evolution of the density matrix is given by $\rho_{_M}(t)$

$$\rho_{_M}(t) = \frac{U(t)\rho_{_M}U(t)^\dagger}{\mathrm{tr}\big(U(t)\rho_{_M}U(t)^\dagger\big)}. \tag{A1}$$

The Pauli decomposition of the density matrix parametrizes the quantum state in terms of the Bloch vector $b_i(t)$

$$\rho_{_M}(t) = \frac{\mathbb{1}_2 + b_i(t)\sigma_i}{2}. \tag{A2}$$

Inverting this equation, one can write the Bloch vector as

$$b_i(t) = \mathrm{tr}\big(\sigma_i\rho_{_M}(t)\big) = \frac{\mathrm{tr}\big(\sigma_i U(t)\rho_{_M}U(t)^\dagger\big)}{\mathrm{tr}\big(U(t)\rho_{_M}U(t)^\dagger\big)} \tag{A3}$$

Using the definition of $U(t)$ from Eq. (5) and taking $p = q = 1/\sqrt{2}$, the explicit from of the Bloch vector is

$$b_x(t) = \frac{b_x\mathrm{ch}_t - \mathrm{sh}_t}{\mathrm{ch}_t - b_x\mathrm{sh}_t}, \qquad b_y(t) = \frac{b_y\mathrm{c}_t + b_z\mathrm{s}_t}{\mathrm{ch}_t - b_x\mathrm{sh}_t}, \qquad b_z(t) = \frac{b_z\mathrm{c}_t - b_y\mathrm{s}_t}{\mathrm{ch}_t - b_x\mathrm{sh}_t}. \tag{A4}$$

where $\mathrm{s}_i = \sin(\Delta m t_i)$, $\mathrm{c}_i = \cos(\Delta m t_i)$, $\mathrm{sh}_i = \sinh(\Delta\Gamma t_i/2)$, $\mathrm{ch}_i = \cosh(\Delta\Gamma t_i/2)$, and $b_i = b_i(0)$ is component of the Bloch vector at $t = 0$. Note that they are normalized by the fraction of the total number of mesons at time t, which is given by

$$\frac{N(t)}{N_0} = \mathrm{tr}\big(U(t)\rho_{_M}U(t)^\dagger\big) = \mathrm{ch}_t - b_x\mathrm{sh}_t \tag{A5}$$

Next we calculate the number distribution of a certain meson state. The ratio of the number of mesons of state $|X\rangle$ at time t over the total number of mesons at $t = 0$ is

$$\frac{N_X(t)}{N_0} = \langle X|U(t)\rho_{_M}U(t)^\dagger|X\rangle = \mathrm{tr}\big(\Pi_X \cdot U(t)\rho_{_M}U(t)^\dagger\big). \tag{A6}$$

where $\Pi_X = |X\rangle\langle X|$ is the projection operator. For flavor eigenstate $X = M$, $\Pi_M = \begin{bmatrix}1 & 0\\ 0 & 0\end{bmatrix}$, for the other flavor eigenstate $X = \bar{M}$, $\Pi_{\bar{M}} = \begin{bmatrix}0 & 0\\ 0 & 1\end{bmatrix}$. Therefore, we can construct the flavor asymmetry and total number as

$$\frac{N_M(t) - N_{\bar{M}}(t)}{N_0} = \mathrm{tr}\Big((\Pi_M - \Pi_{\bar{M}}) \cdot U(t)\rho_{_M}U(t)^\dagger\Big) = \mathrm{tr}\big(\sigma_z \cdot U(t)\rho_{_M}U(t)^\dagger\big) \tag{A7}$$

$$\frac{N_M(t) + N_{\bar{M}}(t)}{N_0} = \mathrm{tr}\Big((\Pi_M + \Pi_{\bar{M}}) \cdot U(t)\rho_{_M}U(t)^\dagger\Big) = \mathrm{tr}\big(\mathbb{1} \cdot U(t)\rho_{_M}U(t)^\dagger\big) \tag{A8}$$

The number distribution of the decayed product f and $\bar{f}$ can be obtained through the definition of decay rate

$$\frac{\mathrm{d}N_{f(\bar{f})}}{\mathrm{d}t} = \Gamma_{M\to f}N_{M(\bar{M})}(t) \tag{A9}$$

where we have used the relation that in the CP conserving case $\Gamma_{M\to f} = \Gamma_{\bar{M}\to\bar{f}}$. Combining Eqs. (A7)−(A9) we find Eqs. (12) and (13).

Appendix B: The Time Evolution of a Pair of Mesons

Defining the unnormalized density matrix for a pair of mesons at time (t_1, t_2) as

$$\mathcal{R}_{_{MM}}(t_1, t_2) \equiv U(t_1) \otimes U(t_2)\,\rho_{_{MM}}\,U^\dagger(t_1) \otimes U^\dagger(t_2), \tag{B1}$$

	B_s^0	B_d^0	D^0	K^0
Γ/ps^{-1}	0.662	0.658	2.44	5.59×10^{-3}
$\Delta m/\Gamma$	26.8	0.769	4.6×10^{-3}	0.95
$\Delta\Gamma/\Gamma$	0.135	4.0×10^{-3}	0.012	1.99

TABLE III. Oscillation and decay parameters for neutral mesons [2, 52, 53].

we can write down the meson numbers similar to Eq. (A7) - (A8)

$$\frac{N_{MM}+N_{\bar{M}M}+N_{M\bar{M}}+N_{\bar{M}\bar{M}}}{N_0} = \text{tr}\Big((\mathbb{1}\otimes\mathbb{1})\cdot\mathcal{R}_{_{MM}}(t_1,t_2)\Big), \tag{B2}$$

$$\frac{N_{MM}-N_{\bar{M}M}-N_{M\bar{M}}+N_{\bar{M}\bar{M}}}{N_0} = \text{tr}\Big((\sigma_z\otimes\sigma_z)\cdot\mathcal{R}_{_{MM}}(t_1,t_2)\Big), \tag{B3}$$

$$\frac{N_{MM}-N_{\bar{M}M}+N_{M\bar{M}}-N_{\bar{M}\bar{M}}}{N_0} = \text{tr}\Big((\sigma_z\otimes\mathbb{1})\cdot\mathcal{R}_{_{MM}}(t_1,t_2)\Big), \tag{B4}$$

$$\frac{N_{MM}+N_{\bar{M}M}-N_{M\bar{M}}-N_{\bar{M}\bar{M}}}{N_0} = \text{tr}\Big((\mathbb{1}\otimes\sigma_z)\cdot\mathcal{R}_{_{MM}}(t_1,t_2)\Big). \tag{B5}$$

To connect to the number distribution of decay products, we again use the definition of decay rate

$$\frac{\mathrm{d}N_{ff}}{\mathrm{d}t_1\mathrm{d}t_2} = \Gamma^2_{M\to f}N_{MM}(t_1,t_2). \tag{B6}$$

Explicitly writing down $\mathcal{R}_{_{MM}}(t_1,t_2)$ using the time evolution operator in Eq. (5) and the expansion of $\rho_{_{MM}}$ in Eq. (14) and calculating the trace, we find the results in Eq. (19) - (22).

Appendix C: Quantum Observables

For a two-qubit system, the concurrence $\mathcal{C}$ [54] is given by

$$\mathcal{C} = \max(0,\lambda_1-\lambda_2-\lambda_3-\lambda_4), \tag{C1}$$

where λ_i $(i=1,2,3,4)$ are the eigenvalues, sorted by decreasing magnitude, of the matrix

$$R_\rho = \sqrt{\sqrt{\rho}\tilde{\rho}\sqrt{\rho}}, \qquad \tilde{\rho} = (\sigma_2\otimes\sigma_2)\rho^*(\sigma_2\otimes\sigma_2). \tag{C2}$$

$0 < \mathcal{C} \leq 1$ indicates an entangled state while $\mathcal{C} = 0$ indicates a separable state. For a separable state, the two subsystems can be fully described independently, but this is not possible for an entangled state.

Bell's inequality is obeyed by all classical theories, including those with local hidden variables [44]. For two qubits, the inequality is given by the CHSH inequality [55]. A state that obeys the CHSH inequality is called Bell local while a state that does not is called Bell nonlocal. The linear approximation to the inequality is measured by the Bell variable $\mathcal{B}$ [21]

$$\mathcal{B} = |C_{yy}+C_{zz}| - \sqrt{2}. \tag{C3}$$

With this normalization, $-\sqrt{2} < \mathcal{B} \leq 0$ indicates a Bell local state and $0 < \mathcal{B} < 2-\sqrt{2}$ indicates a Bell nonlocal state.

Quantum discord $\mathcal{D}$ is the difference between the total mutual information and the classical mutual information. The latter requires an extremization over all possible directions, however, for states where only the correlation matrix

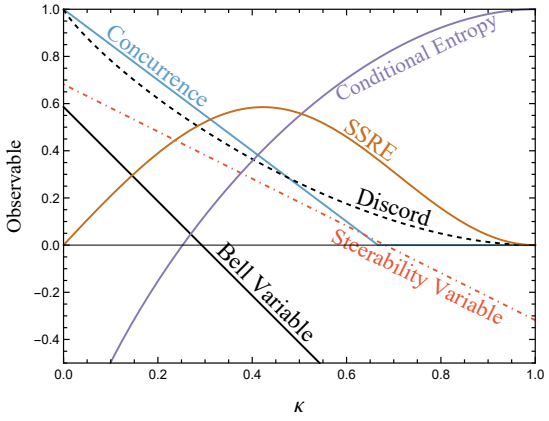

FIG. 2. Representative quantum information quantities versus the parameter κ for Werner states.

is non-zero, there is a closed form [56, 57]

$$\begin{aligned}\mathcal{D} = 1 &+ \frac{1}{4}(1 - C_{zz} - C_{xx} - C_{yy})\log_2\left(\frac{1 - C_{zz} - C_{xx} - C_{yy}}{4}\right) \\ &+ \frac{1}{4}(1 - C_{zz} + C_{xx} + C_{yy})\log_2\left(\frac{1 - C_{zz} + C_{xx} + C_{yy}}{4}\right) \\ &+ \frac{1}{4}(1 + C_{zz} - C_{xx} + C_{yy})\log_2\left(\frac{1 + C_{zz} - C_{xx} + C_{yy}}{4}\right) \\ &+ \frac{1}{4}(1 + C_{zz} + C_{xx} - C_{yy})\log_2\left(\frac{1 + C_{zz} + C_{xx} - C_{yy}}{4}\right) \\ &- \frac{1}{2}(1 + \lambda)\log_2\left(\frac{1 + \lambda}{2}\right) - \frac{1}{2}(1 - \lambda)\log_2\left(\frac{1 - \lambda}{2}\right),\end{aligned} \tag{C4}$$

where $\lambda = \max\{|C_{xx}|, |C_{yy}|, |C_{zz}|\}$. A discord of $\mathcal{D} = 0$ indicates a classical state while a discord of $0 < \mathcal{D} \leq 1$ indicates the presence of quantum correlations.

Bell nonlocality is a relatively strict condition that forbids states with local hidden variable descriptions. A weaker condition is called steerability which forbids states with a description where one subsystem can be described by a local hidden variable theory and the other subsystem can be a quantum theory. The steerability variable $\mathcal{S}$ is given by [58]

$$\mathcal{S} = \frac{1}{2\pi^2}\int \mathrm{d}\hat{\mathbf{n}}\sqrt{\hat{\mathbf{n}}^{\mathrm{T}}\mathbf{C}^{\mathrm{T}}\mathbf{C}\hat{\mathbf{n}}} - \frac{1}{\pi} \tag{C5}$$

where $\mathbf{C}$ is the correlation matrix. When $\mathcal{S} \geq 0$ the state is steerable.

The Von Neumann entropy of a quantum state is defined as

$$S(\rho) = -\mathrm{tr}(\rho\log_2\rho). \tag{C6}$$

The conditional entropy [57, 59] is further defined as

$$S(\rho_{\mathcal{A}}|\rho_{\mathcal{B}}) = S(\rho_{\mathcal{AB}}) - S(\rho_{\mathcal{B}}), \tag{C7}$$

where $\rho_{\mathcal{AB}}$ is the total quantum state of system $\mathcal{A}$ and $\mathcal{B}$, and $\rho_{\mathcal{B}}$ is the reduced density matrix by performing the partial trace over the subsystem $\mathcal{A}$, $\rho_{\mathcal{B}} = \mathrm{tr}_{\mathcal{A}}\rho_{\mathcal{AB}}$.

The second stabilizer Rényi entropy (SSRE) is given by [48]

$$M_2(\rho) = -\log_2\frac{1 + \sum_i (b_i^{\mathcal{A}})^4 + \sum_j (b_j^{\mathcal{A}})^4 + \sum_{i,j} C_{ij}^4}{1 + \sum_i (b_i^{\mathcal{A}})^2 + \sum_j (b_j^{\mathcal{A}})^2 + \sum_{i,j} C_{ij}^2}. \tag{C8}$$

$\mathrm{Br}(M \to f_{\eta_{CP}})$		$\mathrm{Br}(M \to f)$	
$B_d^0 \to J/\psi K_S$	$(8.91 \pm 0.21) \times 10^{-4}$	$B_d^0 \to \ell^+ \nu_\ell X^-$	$(20.66 \pm 0.56)\%$
$B_s^0 \to J/\psi \eta$	$(3.9 \pm 0.7) \times 10^{-4}$	$B_s^0 \to \ell^+ \nu_\ell X^-$	$(19.2 \pm 1.6)\%$
$K_S^0 \to \pi^+\pi^-$	$(69.20 \pm 0.05)\%$	$K_S^0 \to \pi^\pm \ell^\mp \nu_\ell$	$(1.174 \pm 0.01) \times 10^{-3}$
$K_L^0 \to \pi^+\pi^-$	$(1.967 \pm 0.010) \times 10^{-3}$	$K_L^0 \to \pi^\pm \ell^\mp \nu_\ell$	$(67.59 \pm 0.13)\%$

TABLE IV. B^0 and K^0 decay branching fractions adopted in the analyses [2].

Appendix D: Simulations and Experimental Feasibility

To estimate the sensitivity, we first list the branching ratio of the useful channels in Table IV.

[1] M. Gell-Mann and A. Pais, Phys. Rev. **97**, 1387 (1955).
[2] S. Navas *et al.* (Particle Data Group), Phys. Rev. D **110**, 030001 (2024).
[3] A. Apostolakis *et al.* (CPLEAR), Phys. Lett. B **422**, 339 (1998).
[4] F. Ambrosino *et al.* (KLOE), Phys. Lett. B **642**, 315 (2006), arXiv:hep-ex/0607027.
[5] D. Babusci *et al.* (KLOE-2), JHEP **04**, 059 (2022), [Erratum: JHEP 04, 169 (2022)], arXiv:2111.04328 [hep-ex].
[6] A. Go (Belle), J. Mod. Opt. **51**, 991 (2004), arXiv:quant-ph/0310192.
[7] A. Go *et al.* (Belle), Phys. Rev. Lett. **99**, 131802 (2007), arXiv:quant-ph/0702267.
[8] Y.-B. Ding, J.-l. Li, and C.-F. Qiao, (2007), arXiv:hep-ph/0702271.
[9] P. Caban, J. Rembielinski, K. A. Smolinski, Z. Walczak, and M. Wlodarczyk, Phys. Lett. A **357**, 6 (2006), arXiv:quant-ph/0603169.
[10] J. Li and C.-F. Qiao, Phys. Rev. D **74**, 076003 (2006), arXiv:hep-ph/0608077.
[11] T. Ichikawa, S. Tamura, and I. Tsutsui, Phys. Lett. A **373**, 39 (2008), arXiv:0805.3632 [quant-ph].
[12] A. K. Alok and S. Banerjee, Phys. Rev. D **88**, 094013 (2013), arXiv:1304.4063 [hep-ph].
[13] S. Banerjee, A. K. Alok, and R. MacKenzie, Eur. Phys. J. Plus **131**, 129 (2016), arXiv:1409.1034 [hep-ph].
[14] Y. Shi and J. Yang, Phys. Rev. D **98**, 075019 (2018), arXiv:1612.07628 [hep-ph].
[15] Y. Shi and J.-C. Yang, Eur. Phys. J. C **80**, 116 (2020), arXiv:1912.04111 [hep-ph].
[16] Y. Takubo, T. Ichikawa, S. Higashino, Y. Mori, K. Nagano, and I. Tsutsui, Phys. Rev. D **104**, 056004 (2021), arXiv:2106.07399 [hep-ph].
[17] K. Chen, Z.-P. Xing, and R. Zhu, Nucl. Phys. A **1063**, 123199 (2025), arXiv:2407.19242 [hep-ph].
[18] Y. Afik and J. R. M. de Nova, Eur. Phys. J. Plus **136**, 907 (2021), arXiv:2003.02280 [quant-ph].
[19] A. J. Barr, Phys. Lett. B **825**, 136866 (2022), arXiv:2106.01377 [hep-ph].
[20] M. Fabbrichesi, R. Floreanini, and G. Panizzo, Phys. Rev. Lett. **127**, 161801 (2021), arXiv:2102.11883 [hep-ph].
[21] C. Severi, C. D. E. Boschi, F. Maltoni, and M. Sioli, Eur. Phys. J. C **82**, 285 (2022), arXiv:2110.10112 [hep-ph].
[22] R. von Kuk, K. Lee, J. K. L. Michel, and Z. Sun, (2025), arXiv:2503.22607 [hep-ph].
[23] F. Bloch, Phys. Rev. **70**, 460 (1946).
[24] R. P. Feynman, J. Vernon, Frank L., and R. W. Hellwarth, Journal of Applied Physics **28**, 49 (1957), https://pubs.aip.org/aip/jap/article-pdf/28/1/49/18316298/49_1_online.pdf.
[25] F. Roccati, G. M. Palma, F. Bagarello, and F. Ciccarello, Open Systems & Information Dynamics **29**, 2250004 (2022), arXiv:2201.05367 [quant-ph].
[26] D. Karamitros, T. McKelvey, and A. Pilaftsis, Phys. Rev. D **108**, 016006 (2023), [Erratum: Phys.Rev.D 109, 059901 (2024)], arXiv:2212.06031 [hep-ph].
[27] A. K. Alok, S. Banerjee, N. R. S. Chundawat, and S. U. Sankar, JHEP **05**, 124 (2024), arXiv:2402.02470 [hep-ph].
[28] B. O. Kerbikov, Nucl. Phys. A **975**, 59 (2018), arXiv:1704.07117 [hep-ph].
[29] D. Karamitros, T. McKelvey, and A. Pilaftsis, Phys. Rev. D **111**, 096020 (2025), arXiv:2502.15625 [hep-ph].
[30] U. Fano, Rev. Mod. Phys. **55**, 855 (1983).
[31] A. Pich, ICTP Ser. Theor. Phys. **10**, 14 (1994), arXiv:hep-ph/9312297.
[32] G. Buchalla, AIP Conf. Proc. **412**, 49 (1997), arXiv:hep-ph/9707545.
[33] R. F. Werner, Phys. Rev. A **40**, 4277 (1989).
[34] R. Aaij *et al.* (LHCb), Nature Phys. **18**, 1 (2022), arXiv:2104.04421 [hep-ex].
[35] A. Apostolakis *et al.* (CPLEAR), Phys. Lett. B **458**, 545 (1999).
[36] R. Glattauer, PoS **EPS-HEP2015**, 554 (2015).
[37] R. Louvot *et al.* (Belle), Phys. Rev. Lett. **102**, 021801 (2009), arXiv:0809.2526 [hep-ex].
[38] C. Oswald and T. K. Pedlar, Mod. Phys. Lett. A **28**, 1330036 (2013), arXiv:1311.3547 [hep-ex].
[39] D. d'Enterria and A. M. Snigirev, Phys. Rev. Lett. **118**, 122001 (2017), arXiv:1612.05582 [hep-ph].
[40] R. Aaij *et al.* (LHCb), Phys. Rev. D **100**, 031102 (2019), arXiv:1902.06794 [hep-ex].
[41] Y. Afik, Y. Kats, J. R. M. n. de Nova, A. Soffer, and D. Uzan, (2024), arXiv:2406.04402 [hep-ph].
[42] A. Di Domenico, Symmetry **12**, 2063 (2020).
[43] A. Einstein, B. Podolsky, and N. Rosen, Phys. Rev. **47**,

777 (1935).
[44] J. S. Bell, Physics Physique Fizika **1**, 195 (1964).
[45] W. Zurek, Annalen der Physik **512**, 855–864 (2000).
[46] H. Ollivier and W. H. Zurek, Phys. Rev. Lett. **88**, 017901 (2001), arXiv:quant-ph/0105072.
[47] M. Horodecki, J. Oppenheim, and A. Winter, Nature **436**, 673 (2005).
[48] L. Leone, S. F. E. Oliviero, and A. Hamma, Phys. Rev. Lett. **128**, 050402 (2022), arXiv:2106.12587 [quant-ph].
[49] R. A. Bertlmann, A. Bramon, G. Garbarino, and B. C. Hiesmayr, Phys. Lett. A **332**, 355 (2004), arXiv:quant-ph/0409051.
[50] A. Bramon, R. Escribano, and G. Garbarino, J. Mod. Opt. **52**, 1681 (2005), arXiv:quant-ph/0410122.
[51] A. Bramon, R. Escribano, and G. Garbarino, Found. Phys. **36**, 563 (2006), arXiv:quant-ph/0501069.
[52] T. Jubb, M. Kirk, A. Lenz, and G. Tetlalmatzi-Xolocotzi, Nucl. Phys. B **915**, 431 (2017), arXiv:1603.07770 [hep-ph].
[53] Y. S. Amhis *et al.* (HFLAV), Eur. Phys. J. C **81**, 226 (2021), arXiv:1909.12524 [hep-ex].
[54] W. K. Wootters, Phys. Rev. Lett. **80**, 2245 (1998), arXiv:quant-ph/9709029.
[55] J. F. Clauser, M. A. Horne, A. Shimony, and R. A. Holt, Phys. Rev. Lett. **23**, 880 (1969).
[56] S. Luo, Phys. Rev. A **77**, 042303 (2008).
[57] T. Han, M. Low, N. McGinnis, and S. Su, JHEP **05**, 081 (2025), arXiv:2412.21158 [hep-ph].
[58] S. Jevtic, M. J. W. Hall, M. R. Anderson, M. Zwierz, and H. M. Wiseman, J. Opt. Soc. Am. B **32**, A40 (2015).
[59] N. Friis, S. Bulusu, and R. Bertlmann, Journal of Physics A Mathematical and Theoretical **50**, 125301 (2017).